



**HAL**  
open science

# Plasmonic Bipyramidal Au Nanoparticles Enhance Near-Infrared Nonlinear Absorption of Dyes Confined in Sol–Gel Materials: Implications for the Safe Utilization of Lasers

Denis Château, Sylvain David, Gérard Berginc, Cesar Lopes, Frédéric Chaput, Frédéric Lerouge, Anthony Désert, Chantal Andraud, Stephane Parola

## ► To cite this version:

Denis Château, Sylvain David, Gérard Berginc, Cesar Lopes, Frédéric Chaput, et al.. Plasmonic Bipyramidal Au Nanoparticles Enhance Near-Infrared Nonlinear Absorption of Dyes Confined in Sol–Gel Materials: Implications for the Safe Utilization of Lasers. *ACS Applied Nano Materials*, 2022, 5 (3), pp.3773-3780. 10.1021/acsanm.1c04422 . hal-03762391

**HAL Id: hal-03762391**

**<https://hal.science/hal-03762391v1>**

Submitted on 24 Sep 2022

**HAL** is a multi-disciplinary open access archive for the deposit and dissemination of scientific research documents, whether they are published or not. The documents may come from teaching and research institutions in France or abroad, or from public or private research centers.

L'archive ouverte pluridisciplinaire **HAL**, est destinée au dépôt et à la diffusion de documents scientifiques de niveau recherche, publiés ou non, émanant des établissements d'enseignement et de recherche français ou étrangers, des laboratoires publics ou privés.

# Plasmonic Bipyramidal Au Nanoparticles Enhance Near-Infrared Nonlinear Absorption of Dyes Confined in Sol-Gel Materials: Implications for the Safe Utilization of Lasers.

*Denis Château<sup>‡</sup>, Sylvain David<sup>‡</sup>, Gérard Berginc<sup>‡</sup>, Cesar Lopes<sup>§</sup>, Frédéric Chaput<sup>‡</sup>, Frédéric Lerouge<sup>‡</sup>, Anthony Désert<sup>‡</sup>, Chantal Andraud<sup>‡,\*</sup>, Stéphane Parola<sup>‡,\*</sup>*

<sup>‡</sup>Univ. Lyon, Ecole Normale Supérieure de Lyon, Université Claude Bernard Lyon 1, CNRS UMR5182, Laboratoire de Chimie Lyon, 46 allée d'Italie, F69364, France. E-mail: chantal.andraud@ens-lyon.fr, stephane.parola@ens-lyon.fr

<sup>†</sup>Thales LAS France, 2 Avenue Gay Lussac, 78990 Élancourt, France.

<sup>§</sup>Electrooptical Systems, Swedish Defence Research Agency (FOI) Linköping SE-581 11, Sweden.

KEYWORDS (Nonlinear optics, Optical limiting, sol-gel, plasmonic, azabodipy, SWIR).

ABSTRACT. The increasing use of lasers in many different fields, from UV to NIR wavelengths, requires the development of efficient broadband optical protections to ensure safety during their utilizations. Among the available technologies, nonlinear optical limiting appears as the most

versatile and efficient one. Earlier research has focused on optical limiting materials for visible wavelengths. NIR wavelengths used in telecommunication or optical sensors such as for autonomous vehicles, represent a highly challenging area with very few reports in particular in the solid-state. This work discusses the preparation of efficient NIR optical filter combining azobipy dyes with plasmonic nanoparticles in sol-gel monoliths. The strategy allows to strongly enhance the nonlinear performance of the dyes, creating a synergy effect never observed on such system in the NIR.

## INTRODUCTION.

The development of lasers in the 60s gave rise to intense research programs in optics and nonlinear optics.<sup>1</sup> This has led to a broad range of available continuous or pulsed lasers, ranging from the UV to the NIR wavelengths. They are used in many different fields, from data storage to telecommunications, and for instance in telemetry for airplanes or cars to detect other vehicles or obstacles. One drawback is the requirement for optical protection to ensure a safe utilization of the commercially available lasers. An efficient protection technology emerged which is based on nonlinear optical limiters.<sup>2,3</sup> Nonlinear optical limiters can possess extremely fast activation times, low laser clamping values and high damage thresholds. Reverse Saturable Absorption and Multiphoton Absorption are among the most efficient processes to achieve nonlinear optical limiting.<sup>4</sup>  
<sup>12</sup> During the past 20 years, numerous publications report efficient nonlinear optical limiting dyes in the visible and in the near infrared wavelengths (NIR).<sup>13</sup> Even if some of them are efficient in solution, there is a requirement for integration into solid materials to fulfill the field application criteria.<sup>14,15</sup> Regarding the design of solid-state materials, publications are remaining scarce and essentially limited to visible wavelengths.<sup>5,13,16</sup> While some approaches report thin film materials,<sup>17-21</sup> the use of 3D monolithic materials appears as a credible alternative to thin films

since they allow better localisation of the focal point in the core of the active material. Most of the reported monolithic materials, for visible wavelengths applications are based on organic polymers,<sup>5,8,22-26</sup> sol-gel hybrid glasses<sup>27-38</sup> or sodium–zinc borate glass doped with gold nanoparticles. To the best of our knowledge the two only reports on 3D monolithic solid-state nonlinear optical limiters, operating in the short-wave infrared (SWIR), which is a promising range for the development light detection and ranging (LIDAR) systems working at the eye safe wavelength of 1550 nm, are by our group, on sol-gel derived materials.<sup>39-40</sup> In most cases, silica based matrices are favoured over organic polymer matrices due to higher damage threshold and nonlinear parameters ( $n_2$ ,  $\beta$ ,  $Re[\chi^{(3)}]$ ,  $Im[\chi^{(3)}]$ ).<sup>16,41</sup> Low compatibility and solubility of dyes in the sol-gel host matrices is often a limitation since the optical performances are concentration dependent. This limitation can be overcome by silanization of dopants to highly improve their concentration through strong covalent bonding between the dyes and the matrix.<sup>30,32,33,40,42-44</sup> Another alternative to improve the optical performance is to use plasmon enhanced optical limiting. This strategy has already proven to be of high efficiency in the visible wavelength but has never been demonstrated so far in the SWIR.<sup>37</sup> Based on these earlier findings, the intention was set on combining a dye and a plasmonic nanostructure in a solid host for SWIR applications. Silica based sol-gel materials are therefore selected as hosting matrices as they have proven to give highly efficient optical power limiting materials, both in the visible and SWIR.<sup>34,39,40</sup> Combining plasmonic nanostructures with the dyes, in the glass material, previously allowed an enhancement of two-photon absorption especially at the wavelengths where it is weak.<sup>37</sup> Similar strategy transferred to the SWIR is not trivial. It requires the use of stable metal nanoparticles with longitudinal plasmon resonances above 1.5  $\mu\text{m}$ , dispersability and stabilisation in a hybrid glass together with an adapted SWIR chromophore.

Herein, we investigate the synergy between conjugated aza-bodipy dyes and plasmonic nanostructures for optical power limiting application in the SWIR. Aza-bodipy dyes, **1** (Figure 1) functionalized by the dialkylaminophenylethynyl in the 1,8 positions is known to present good nonlinear optical properties (nonlinear absorption induced by two-photon absorption and followed by excited state absorption) in the SWIR and particularly at 1.5 $\mu\text{m}$ .<sup>45</sup> These dyes also present the chemical inertness to be successfully incorporated in a bulk xerogel, which gave rise to the first solid-state optical power limiting material at 1.5 $\mu\text{m}$  reported in the literature so far.<sup>39,40</sup> Nanobipyramidal gold structures (AuBPs, figure 1) are considered in this work for the synergy enhancement of optical power limiting of the Aza-bodipy dyes, since they allow very precise tuning of the plasmon resonance in the visible and in the SWIR region. They also have intense longitudinal resonances which is located in the SWIR and hot spots at the tips.<sup>46-48</sup> Moreover, they are stable and can easily be incorporated in a sol-gel matrix such as previously demonstrated.<sup>37,49</sup> The synthesis of the hybrid sol-gel monolith, co-doped with dye **1** and various concentrations of AuBPs, is described here and the materials are optically fully characterized.

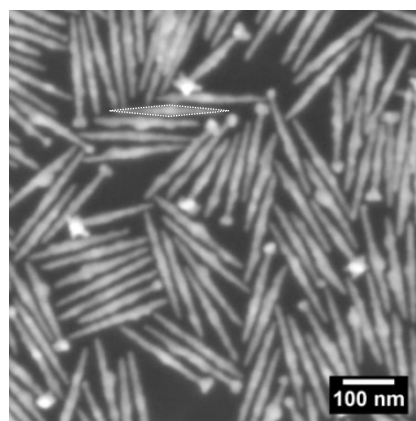
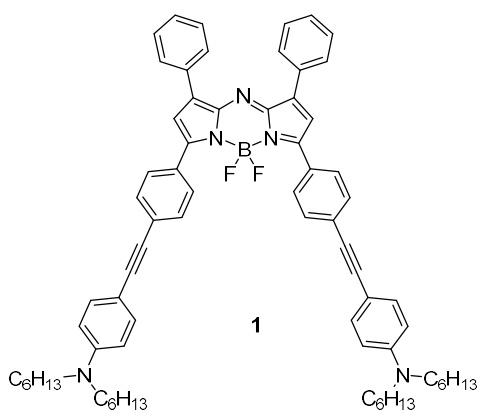


**Figure 1.** Structure of the functionalized azabodipy dye **1** and SEM images of the plasmonic nanostructures *AuBPs@1730nm* (the outline of one of the particles is enhanced with a dotted line to show the bipyramidal shape).

## RESULTS AND DISCUSSION.

**The Aza-Bodipy and the plasmonic NPs.** The Azabodipy **1** has an intense and broad absorption band in the visible (Figure 2). In the NIR a broad transition centered at 740 nm with a cut-off wavelength of 865 nm and a red-tail close to 1000 nm is observed, as previously described in ref. 45. The compound also exhibits two-photon absorption properties in the SWIR band between 1100 and 1600 nm, with a maximum at 1150 nm and a less intense band at around 1500 nm.<sup>45</sup> Detailed photophysical studies indicate that the contribution of the charge transfer transition from the dialylamino-donor group to the central azabodipy core, acting as an electron withdrawing moiety, is responsible for the position and intensity of the nonlinear response.<sup>49</sup> The molecule is also known to present straightforward optical limiting properties in solution and in a sol-gel matrix.<sup>39,40,50</sup>

The AuBPs are prepared according to the reported procedure.<sup>48</sup> Few of the particles present small star-shaped excrescences at the tips, which is a common defect encountered for very elongated Au bipyramids, but as shown in Figure 2, this does not affect the plasmon absorption bands significantly. The overall background absorbance of the bipyramids below 1000-1200nm is slightly increased as shown by the comparison between the spectra of defect free bipyramids from Chateau et al. compare to the one used in this study.<sup>37</sup>

The AuBPs are functionalized with a thiolated silicone oligomer (Figure 3),<sup>37,51</sup> to improve the dispersability and stability of the particles in the hybrid silicon precursor sol. The chosen AuBPs

have a main Surface Plasmon Resonance (SPR) absorption centered at 1730 nm and an aspect ratio close to 10 (mean particle size of 20 x 205nm). Thus, the AuBPs has no or very low SPR absorption in the spectral range 1200 – 1500 nm (the range of interest, ROI) where **1** is NLO active (Figure 2). Consequently, in the ROI, the linear absorption of all components is relatively low.

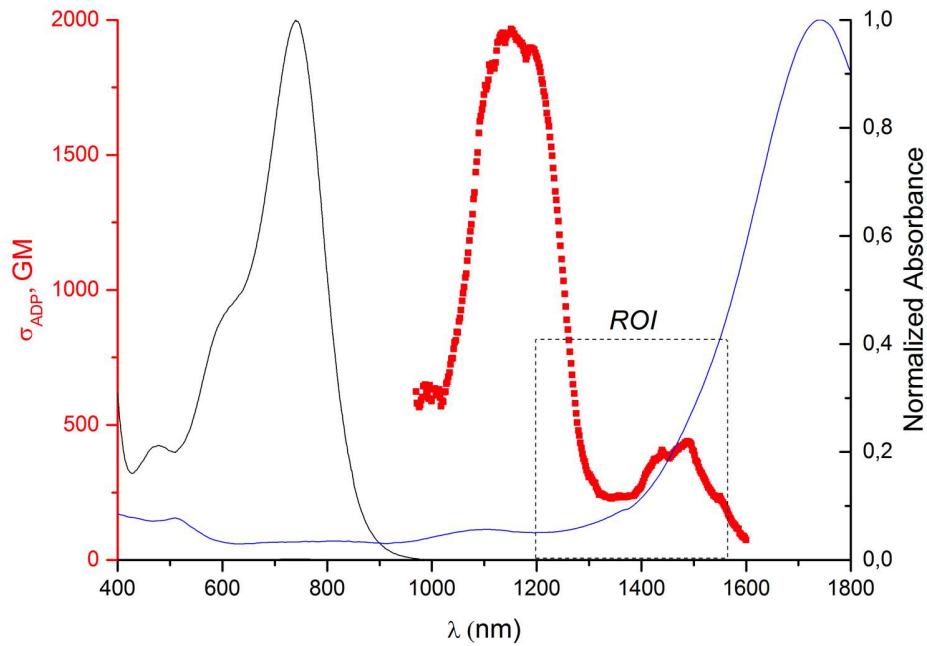


**Figure 2.** Overlay of normalized 1PA in dichloromethane (black) with 2PA (black squares) in carbon tetrachloride spectra of dye **1**<sup>16</sup> and AuBP@1730 (blue) in water.

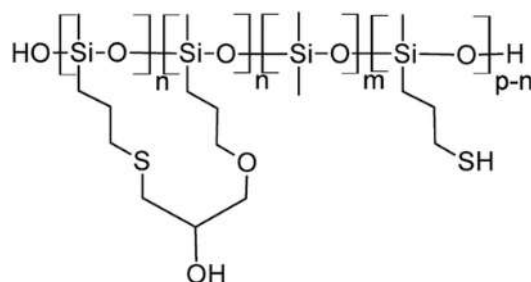
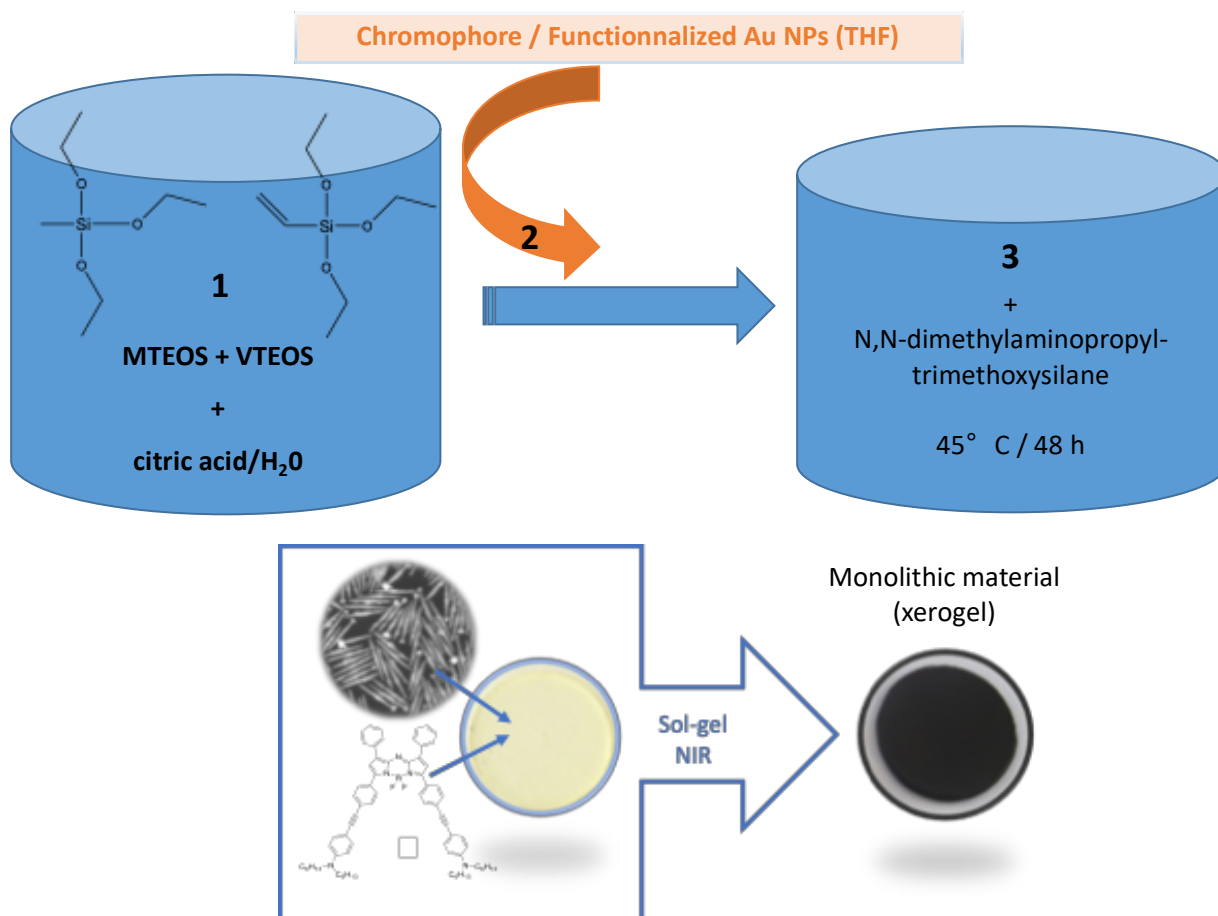


**Figure 3.** Schematic representation of the thiolated silicone oligomer designed for functionalization of the AuBPs.<sup>91</sup>

**Sol-Gel monoliths.** In order to study the influence of the AuBPs on the NLO properties of dye **1**, both particles and dyes need to be homogeneously dispersed in the transparent sol-gel matrix. The procedure that was successfully used in the visible with platinum acetylide dyes and gold nanoparticles cannot be applied straightforward here since the dye is pH sensitive.<sup>37,39</sup> Thus the procedure is modified and a hybrid sol is prepared from the citric acid catalyzed hydrolysis of a mixture of methyltriethoxysilane (MTEOS) and vinyltriethoxysilane (VTEOS) in a 50:50 molar ratio (Scheme 1). The presence of VTEOS limits the formation of micropores that may induce oxygen trapping or diffusion and consequently loss of optical properties.<sup>34</sup>



Scheme 1. Overview of the process used for the preparation of the hybrid materials.

The sol is thoroughly washed to remove the acid catalyst and partially neutralize the product. The sol has a high hydrophobic character and a high condensation ratio (close to 85% based on liquid  $^{29}\text{Si}$  NMR) enabling the introduction of the dopants dissolved in THF. The final condensation is catalyzed by N,N-dimethylaminopropyltrimethoxysilane which is, thus, used as a gelation agent. The use of a tertiary amine is more convenient than the previously reported trimethoxysilane, which induces hydrogen formation and therefore possible trapping of gas bubbles during the gelification.<sup>39</sup> This substitution avoids bubbles being trapped in the final solid material, which represents an important improvement of the initial process.

The co-doped monolithic xerogels are obtained by dissolving dye **1** in a minimal volume of THF and mixing with the sol. Then, the suspension of gold NPs in THF and the gelation agent are added. The monolithic material is obtained after 2 days aging at 45°C in a mold. Xerogels with AuBP but without dye were also prepared later to verify the impact of the AuBP on the OPL performance. Overall, seven monoliths containing dyes **1** (5 wt%) and the NPs at different concentrations were prepared (Table 1). After demolding, dark monolithic discs of 1.2 cm diameter and 0.3 cm thickness are obtained (Figure 4).

**Table 1.** Composition of the monoliths doped with chromophore **1** and gold NPs.

Material reference	Chromophore		Gold nanobipyramids	
	Concentration		AuBP	
	%wt	mM	LSPR (nm) <sup>a)</sup>	[AuBP] (nM)
<b>MIt-1 (reference)</b>	5%	56	n/a	n/a

<b>Mlt-2</b>	5%	56	1730	0,04
<b>Mlt-3</b>	5%	56	1730	0,08
<b>Mlt-4</b>	5%	56	1730	0,16
<b>Mlt-5</b>	n/a	n/a	1630	0,04
<b>Mlt-6</b>	n/a	n/a	1630	0,08
<b>Mlt-7</b>	n/a	n/a	1630	0,16

<sup>a)</sup>LSPR measured in water dispersions



**Figure 4.** Different monoliths (from left to right, diameter 13 mm): **Mlt-1** doped with dye **1** (5% wt) and **Mlt-3** co-doped with dye **1** (5% wt) and AuBP@1730 (0.08 nM).

*Optical Characterization of monoliths.* High optical quality of the prepared glasses (**Mlt-1-7**) is required to undertake NLO measurements, since any surface or bulk inhomogeneity (aggregate, phase segregation...) immediately results in strong linear absorption or scattering of the incident laser. The monoliths are therefore polished to high optical quality and their optical transmission is verified (Figure 5 and Figure 6, left). All dye doped materials are opaque below 1000 nm, corresponding to the red-tail of the absorption of dye **1** present in the material (5 wt%). In the ROI (1200-1600 nm), all dye doped materials except Mlt-4 present a very good transparency with an average transmission of 75-90 %.

However, the overall linear transmission tends to decrease within ROI with an increase in AuBPs concentration (Figure 5). This can be attributed to the tail of longitudinal SPR band and also from its broadening due to a partial aggregation of NPs at the highest concentrations. Substraction of the matrix/dye spectrum from MIt-3 reveals the clear presence of the AuBP longitudinal SPR band (Figure S1) with a red-shift and a visible broadening compared to the AuBP in water. This confirms the presence of dispersed AuBP in the co-doped xerogels, as complete aggregation would result in no visible SPR peak, but also indicates an influence of the dye **1** on the quality of the dispersion.

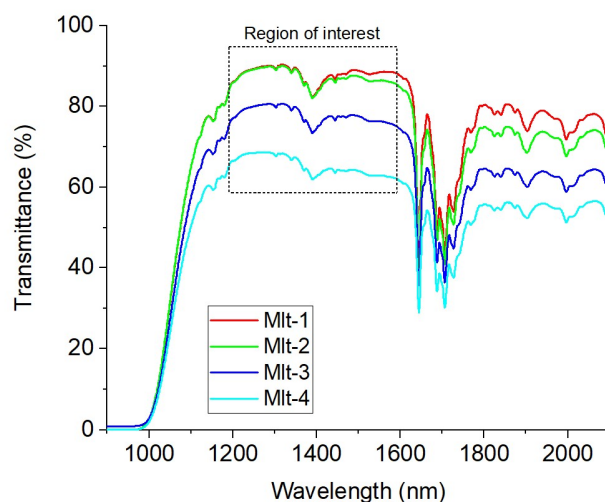


**Figure 5.** Transmission spectra of the dye doped monoliths. The spectral region of interest (ROI) is marked, dashed line.

On the other hand, the xerogels doped only with AuBP (Figure 6) show the transverse SPR band (at 510 nm) and a slightly blue-shifted longitudinal SPR band (at 1605 nm), compared to the particles in solution at 510 and 1630 nm respectively (see Figure S2). This slight blue-shift indicates a small alteration of the tips of the nanoparticles but no significant degradation of the

nanoparticles caused by the incorporation into the sol-gel matrix. The thin LSPR band also indicates minimal aggregation compared to the dye-doped materials.

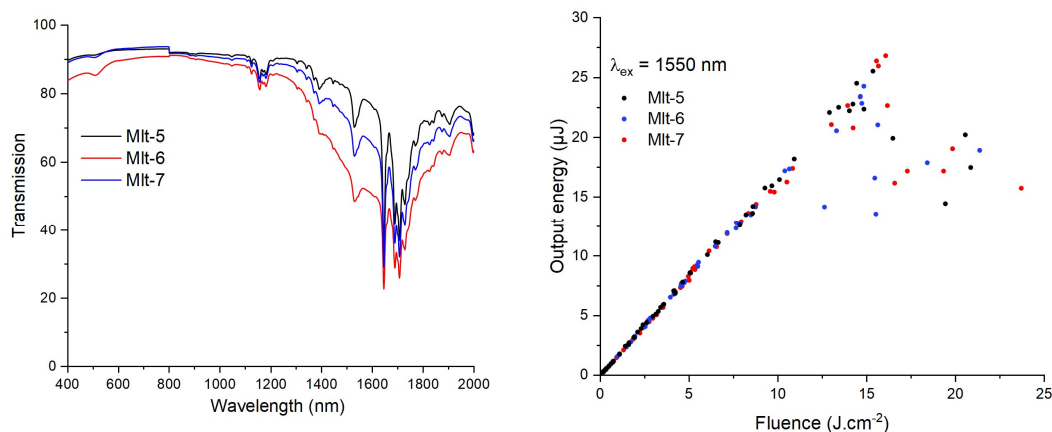


**Figure 6.** Left: Linear transmission of glass materials **MIt-5** to **MIt-7**. Right: Optical limiting of **MIt-5** to **MIt-7** doped solely with Au nanoparticles at concentrations of 0.04, 0.08 and 0.16 nM at 1500 nm.

**Optical power limiting.** Figure 6 right displays the OPL curves of **MIt-5** - **MIt-7** glasses doped with only AuBPs at different concentrations. There is a lack of OPL response for the materials. The reduction in transmission with an increased fluence originates from laser induced damage (even though the glasses were moved in a direction perpendicular to the laser beam after each shot). This allows to exclude the direct role of NPs in the OPL efficiency of the chromophores in the co-doped systems and to discuss it in terms of plasmonic coupling between both moieties.

Figure 7 compares the OPL data of the two doped glasses, the reference material, **MIt-1**, (with a dye concentration of 56 mM) and **MIt-3** (with a concentration of 56 mM and 0,08 nM for dye **1** and AuBPs, respectively). For all incident wavelengths (1200, 1300, 1400, 1550 nm), an important

improvement of the OPL response is observed, with a significant decrease of the clamping level compared to the reference (glass material doped solely with the dye). The strongest effect occurs at 1550 nm (Figure 7): an optical limiting clamping of the transmitted intensity at 30  $\mu\text{J}$  is measured against 50  $\mu\text{J}$  for the sample without any NPs, while the plasmon resonance presents the highest value among the four incident studied laser wavelengths. This observation illustrates the relevant role in optical limiting properties of plasmonic NPs.

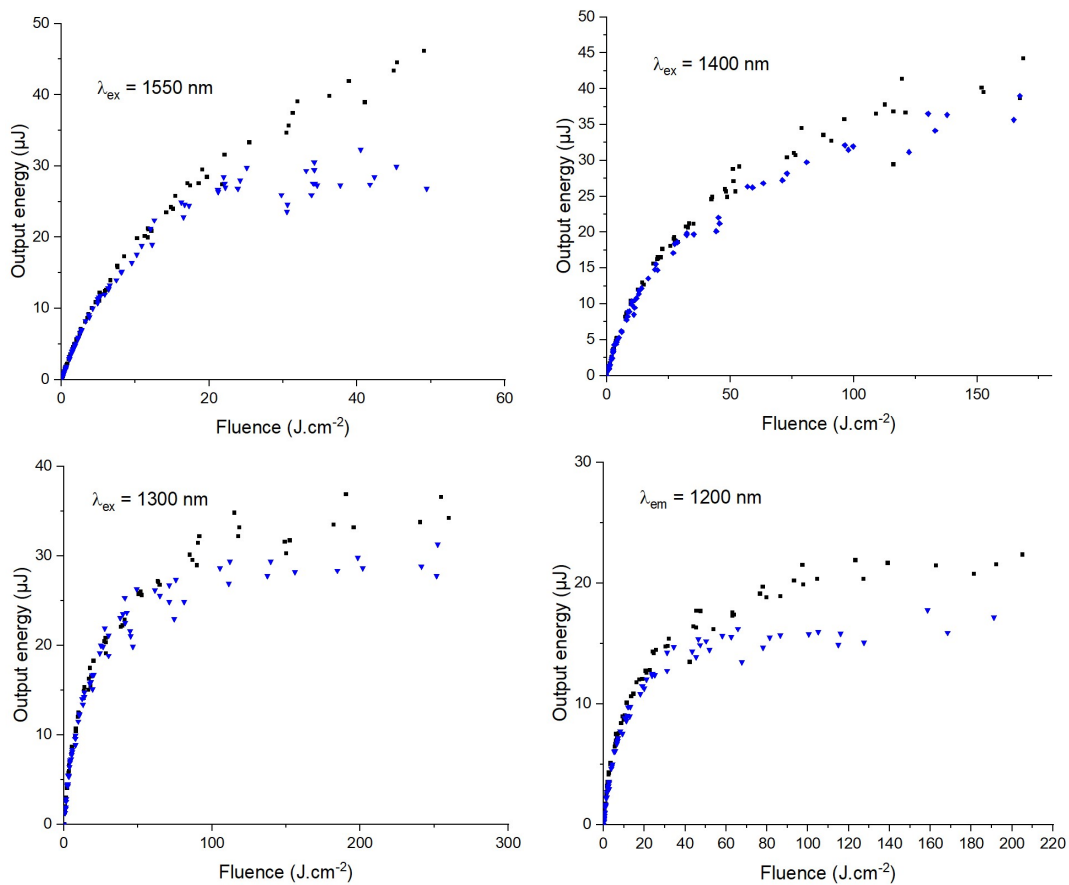


**Figure 7.** Optical Limiting of MIt-1 (black dots) and MIt-3 (blue dots) at 1550, 1400, 1300 and 1200 nm wavelength.

The role of the concentration of NPs is also evaluated. Monoliths with concentrations of 56 mM in dyes and various concentrations of NPs are optically evaluated (Figure 8). In the OPL measurements, on the different glasses, it appears that the clamping level decreases from 35  $\mu\text{J}$  to 20  $\mu\text{J}$  when the NPs concentration increases (Figure 8 center). However, when normalized OPL is drawn considering the linear transmission (Figure 8 left), obviously the most efficient enhancement appears to be at the lowest concentration in NPs (Figure 8 right). This observation is due to the increase in linear absorption at 1550 nm related to the plasmon intensity, screening out the nonlinear absorption effect, while the overall effect combining both linear and nonlinear absorption appears as more efficient. This is consistent with results previously observed for visible wavelengths.<sup>37</sup>

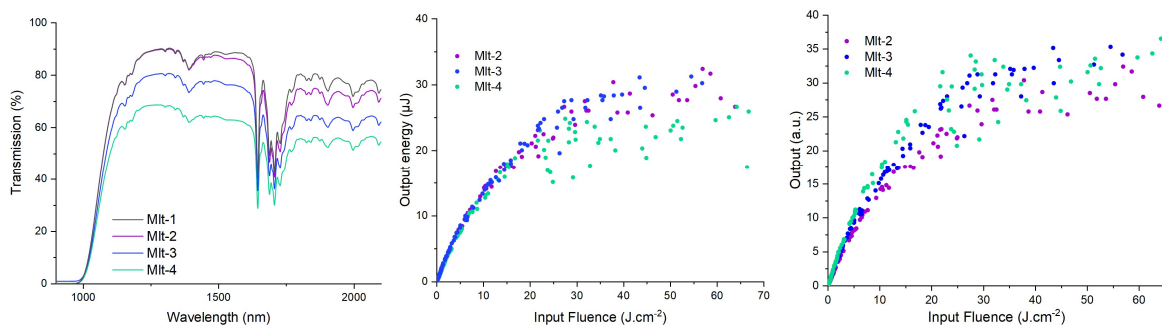


**Figure 8.** Transmission spectra, OPL and normalized OPL (respectively from left to right) of monoliths with concentrations of 56 mM in dye and 0.04, 0.08 and 0.16 nM in AuNPs (**MIt-2** to **MIt-4**) (Exc. 1550 nm).

## CONCLUSIONS

Monolithic sol-gel hybrid plasmonic materials for nonlinear absorption, displaying unprecedented optical performances at SWIR wavelengths are reported. The results originate from the combination of an NLO efficient dye in the 1200-1600 nm wavelength range and an elongated

plasmonic nanostructure with longitudinal resonance in the similar NIR range, having appropriate absorption overlap. Several hybrid monolithic glasses with different NPs concentrations are prepared in the range 0.04 - 0.16 nM and co-doped glasses, containing the dye and NPs. The co-doped glasses show high linear transmission properties in the ROI and a strong enhancement of the nonlinear absorption, leading to a decrease in the optical limiting clamping levels up to 40%, for all measured wavelengths. The enhancement is most pronounced for the lowest used concentration of the NPs. These results expand concepts recently discovered in the visible wavelengths towards the more challenging SWIR region and represent a valuable method to optimize NLO materials using field enhancement mechanisms that can be used for efficient optical protections.

## MATERIALS AND METHODS

Methyltriethoxysilane (MTEOS, 98%), vinyltriethoxysilane (VTEOS, 99%) and N,N-dimethylaminopropyltrimethoxysilane were ordered from ABCR. Tetrachloroauric acid trihydrate (99,99%) was ordered from Alfa Aesar. Citric acid (99%), cetyltrimethylammonium bromide (CTAB, 99%) and cetyltrimethylammonium chloride (CTAC, 25%wt aqueous solution) were ordered from Sigma-Aldrich. TWEEN 80 (also named Polysorbate 80, no purity mentioned) was ordered from Acros.

**Gold bipyramids synthesis.** Gold pentatwinned seeds are prepared as described in the literature.<sup>48</sup> A growth solution is prepared by dissolving 8 mg of CTAB (for a LSPR around 1700) in 12 ml of CTAC solution (140 mM in water) and adding 120  $\mu$ l of HAuCl<sub>4</sub> (25 mM in water). Then 90  $\mu$ l of aqueous silver nitrate (5 mM) are added, followed by 120  $\mu$ l of 8-hydroxyquinoline (0.4 M solution in ethanol). The growth solution turns light yellow. After 2 minutes, 80  $\mu$ l of gold

seeds are then quickly introduced into the growth solution. The mixture is gently stirred for ten seconds and directly put into an oven at 40-45°C for 20 minutes. Then, 80 µl of HQL (0,4 M in ethanol) is added to the mixture and left for 45 minutes at 40-45°C. Finally, 1 ml of a 10% TWEEN80 solution is then added to improve the colloidal stability of the particles and the mixture is kept at 45 °C for an additional 45 minutes. The resulted particles are purified by centrifugation at 6000 rpm and redispersed into 12ml of 3mM CTAC to yield a suspension at 0,25 mM in Au<sup>0</sup> and 0,16 nM of AuBP. The final particles are then functionalized and transferred to THF (maintaining the same concentration) just before use, according to the literature.<sup>51</sup>

**MTEOS/VTEOS sol synthesis.** An equimolar mixture of MTEOS (50 ml) and VTEOS (53 ml) is hydrolyzed using a 15g/l citric acid solution in water. The hydrolysis molar ratio water/precursor is h=11. The mixture is stirred overnight at 25°C. The resulting mixture is evaporated under vacuum to remove the ethanol formed during hydrolysis, allowing the decantation of a hydrophobic phase, rich of hydrolyzed and condensed MTEOS. This phase is dissolved in diethyl ether (150 ml) to remove residual water after phase separation. The resulting organic phase is washed thoroughly four times with water (30 ml each time) to remove traces of citric acid and thereby reach pH above 4.5. Then diethyl ether is evaporated and replaced by THF. Evaporation of the solvents gives a dried solid residue with 45 % in mass. This prepared sol can be stored at -24°C and kept for several months.

**Sol-gel monolith preparation.** Typically, in a PFA mold, 17 mg of dye 1 is introduced and dissolved in 100-150µl of THF. After complete dissolution, 700 mg of the previously prepared MTEOS/VTEOS sol are introduced, followed by the desired amount of AuBP suspension in THF (0, 75, 150 or 300µl for 0, 0.04, 0.08 and 0.16 nM of AuBP in the final material respectively) and completed to around 1ml volume with THF. 30 µl of N,N-dimethylaminopropyltrimethoxysilane

is added to the mixture in the mold. The mold is closed with a screw cap, that has a small hole (x mm), and manually stirred for 30s and then kept undisturbed at room temperature until gelation occurs (typically around 20-30 min). The gelified material is put in an oven at 45°C for 2 days to yield the final xerogel.

**Polishing of the glass materials.** A Struers polishing equipment (Struers LaboPol-25) was used. The final polished materials had a thickness of  $1 \pm 0.05$  mm.

**Optical characterization.** Transmittance spectra were recorded with a CARY 5000 UV-Vis-NIR spectrophotometer. The OPL measurement set-up, which has been described earlier,<sup>52</sup> is based on a  $f/5$  system. The laser beam (source an EKSPLA NT342C OPO, emitting 5 ns pulses) is expanded by a 3x Keplerian telescope. The beam passes through a pinhole filter with 25  $\mu\text{m}$  diameter, placed between two  $f=20$  cm lenses, for beam clean up, leading to a pellicle beam splitter that sends a small part of the pulse energy to the reference detector. The remaining pulse energy is expanded by a 2.66x Keplerian telescope and passed through a 2 cm aperture creating an approximately top-hat beam, which reaches a 2.5 x Keplerian telescope that forms the  $f/5$  system. A simple plano-spherical lens of focal length 1m is used to focus the transmitted beam onto the signal pulse energy detector. The system is aligned at 1550 nm with the help of a digital video camera and a small aperture placed after the plano-spherical lens. For other wavelengths the 1550 nm alignment is used while transposing the front lens of the  $f/5$  telescope to maximize the transmission through the last aperture. The beam diameter, for all the used wavelengths, was measured with the 10-90% knife-edge method. The beam diameter varied between 16 and 25  $\mu\text{m}$  depending on the wavelength.

ASSOCIATED CONTENT

**Supporting Information.** Absorption spectra of AuBP and sol-gel materials are available as Supporting Information.

## AUTHOR INFORMATION

### Corresponding Author

Prof. S. Parola,  
Univ. Lyon, Ecole Normale Supérieure de Lyon, Université Claude Bernard Lyon 1, CNRS UMR5182, Laboratoire de Chimie Lyon, 46 allée d'Italie, F69364 , France.  
E-mail: [stephane.parola@ens-lyon.fr](mailto:stephane.parola@ens-lyon.fr)

Dr. C. Andraud,  
Univ. Lyon, Ecole Normale Supérieure de Lyon, Université Claude Bernard Lyon 1, CNRS UMR5182, Laboratoire de Chimie Lyon, 46 allée d'Italie, F69364 , France.  
E-mail: [chantal.andraud@ens-lyon.fr](mailto:chantal.andraud@ens-lyon.fr)

### Author Contributions

The manuscript was written through contributions of all authors. All authors have given approval to the final version of the manuscript.

## ACKNOWLEDGMENT

Hampus Lundén is thanked for participation in the OPL measurements. SP acknowledges Région Auvergne Rhône-Alpes for financial support (Project HYPOLASE).

## REFERENCES

- (1) Maiman, T. H. Stimulated Optical Radiation in Ruby. *Nature* **1960**, *187*, 493-494.
- (2) Hollins, R. C. Materials for optical limiters. *Curr. Opin. Solid State Mat. Sci.* **1999**, *4*, 189-196.

- (3) Spangler, C. W. Recent development in the design of organic materials for optical power limiting. *J. Mater. Chem. A* **1999**, *9*, 2013-2020.
- (4) Dini, D.; Calvete, M. J.; Hanack, M. Nonlinear Optical Materials for the Smart Filtering of Optical Radiation. *Chem. Rev.* **2016**, *116* (22), 13043-13233.
- (5) Bouit, P.-A.; Maury, O.; Feneayrou, P.; Parola, S.; Kajzar, F.; Andraud, C. in *Multiphoton processes in organic materials and their applications*, (Eds: Rau I., K. F), Archives Contemporaines & Old City Publishing, Paris – Philadelphia, **2011**, 275.
- (6) McKay, T. J.; Bolger, J. A.; Staromlynska, J.; Davy, J. R. Linear and nonlinear optical properties of platinum-ethynyl. *J Chem Phys* **1998**, *108*, 5537-5541.
- (7) He, G. S.; Bhawalkar, J. D.; Zhao, C. F.; Prasad, P. N. Optical limiting effect in a two-photon absorption dye doped solid matrix. *Appl. Phys. Lett.* **1995**, 2433-2435.
- (8) He, G. S.; Gvishi, R.; Prasad, P. N.; Reinhardt, B. A. Two-photon absorption based optical limiting and stabilization in organic molecule-doped solid materials. *Opt. Commun.* **1995**, *117*, 133-136.
- (9) Ehrlich, J. E.; Wu, X. L.; Lee, I. Y. S.; Hu, Z. Y.; Rockel, H.; Marder, S. R.; Perry, J. W. Two-photon absorption and broadband optical limiting with bis-donor stilbenes. *Opt Lett* **1997**, *22*, 1843-1845.
- (10) Reinhardt, B. A.; Brott, L. L.; Clarson, S. J.; Dillard, A. G.; Bhatt, J. C.; Kannan, R.; Yuan, L. X.; He, G. S.; Prasad, P. N. Highly Active Two-Photon Dyes: Design, Synthesis, and Characterization toward Application. *Chem. Mater.* **1998**, *10*, 1863-1874.

- (11) Li, C. F.; Zhang, L.; Yang, M.; Wang, H.; Wang, Y. X. Dynamic and steady-state behaviors of reverse saturable absorption in metallophthalocyanine. *Phys. Rev. A* **1994**, *49*, 1149-1157.
- (12) Perry, J. W.; Mansour, K.; Lee, I. Y. S.; Wu, X. L.; Bedworth, P. V.; Chen, C. T.; Marder, D. N. S. R.; Miles, P.; Wada, T.; Tian, M.; Sasabe, H. Organic optical limiter with a strong nonlinear absorptive response. *Science* **1996**, *273*, 1533-1536.
- (13) He, G. S.; Tan, L.-S.; Zheng, Q.; Prasad, P. N. Multiphoton Absorbing Materials: Molecular Designs, Characterizations, and Applications. *Chem. Rev.* **2008**, *108*, 1245-1330.
- (14) Miller, M. J.; Mott, A. G.; Ketchel, B. P. General Optical Limiting Requirements. *Proc. SPIE* **1998**, *24*, 3472 ; Miles, P. A. Bottleneck optical limiters: the optimal use of excited-state absorbers. *Appl. Opt.* **1994**, *33*, 6965-6979.
- (15) Justus, B. L.; Huston, A. L.; Campillo, A. J. Broadband thermal optical limiter. *Appl. Phys. Lett.* **1993**, *63*, 1483-1486.
- (16) Parola, S.; Julian-Lopez, B.; Carlos, L. D.; Sanchez, C. Optical Properties of Hybrid Organic-Inorganic Materials and their Applications. *Adv. Funct. Mater.* **2016**, *26* (36), 6506-6544.
- (17) Doyle, J. J.; Wang, J.; O'Flaherty, S. M.; Chen, Y.; Slodek, A.; Hegarty, T.; Carpenter II, L. E.; Wöhrle, D.; Hanack, M.; Blau, W. J. Nonlinear optical performance of chemically tailored phthalocyanine-polymer films as solid-state optical limiting devices. *J. Opt. A: Pure Appl. Opt.* **2008**, *10*, 075101.
- (18) Su, X.; Xu, H.; Deng, Y.; Li, J.; Zhang, W.; Wang, P. Preparation and optical limiting properties of a POSS-containing organic-inorganic hybrid nanocomposite. *Mater. Lett.* **2008**, *62*, 3818-3820.

- (19) Su, X.; Guang, S.; Xu, H.; Yang, J.; Song, Y. The preparation and optical limiting properties of POSS-based molecular hybrid functional materials. *Dyes Pigments* **2010**, *87*, 69-75.
- (20) Su, X.; Guang, S.; Li, C.; Xu, H.; Liu, X.; Wang, X.; Song, Y. Molecular hybrid optical limiting materials from polyhedral oligomer silsesquioxane: Preparation and relationship between molecular structure and properties. *Macromolecules* **2010**, *43*, 2840-2845.
- (21) Manthrammel, M. A.; Aboraia, A. M.; Shkir M.; Yahia, I. S.; Assiri, M. A.; Zahran, H. Y.; Ganesh, V.; AlFaify, S.; Soldatov, A.V. Optical analysis of nanostructured rose bengal thin films using Kramers–Kronig approach: New trend in laser power attenuation. *Optics & Laser Technology* **2019**, *112*, 207-214.
- (22) Jiang, H.; De Rosa, M. E.; Su, W.; Brant, M. C.; McLean, D. G.; Bunning, T. J. Polymer host materials for optical limiting. *Proc. SPIE* **1998**, *3472*, 157.
- (23) Westlund, R.; Malmström, E.; Lopes, C.; Öhgren, J.; Rodgers, T.; Saito, Y.; Kawata, S.; Glimsdal, E.; Lindgren, M. Efficient Nonlinear Absorbing Platinum(II) Acetylide Chromophores in Solid PMMA Matrices. *Adv. Func. Mater.* **2008**, *18*, 1939-1948.
- (24) Price, R. S.; Dubinina, G.; Wicks, G.; Drobizhev, M.; Rebane, A.; Schanze, K. S. Polymer Monoliths Containing Two-Photon Absorbing Phenylenevinylene Platinum(II) Acetylide Chromophores for Optical Power Limiting. *ACS Appl. Mater. Interfaces* **2015**, *7*, 10795-10805.
- (25) Ouyang, Q.; Xu, Z.; Lei, Z.; Dong, H.; Yu, H.; Qi, L.; Li, C.; Chen, Y. Enhanced nonlinear optical and optical limiting properties of graphene/ZnO hybrid organic glasses. *Carbon* **2014**, *67*, 214-220.
- (26) Ouyang, Q.; Yu, H.; Xu, Z.; Zhang, Y.; Li, C.; Qi, L.; Chen, Y. Synthesis and enhanced nonlinear optical properties of graphene/CdS organic glass. *Appl. Phys. Lett.* **2013**, *102*, 031912.

- (27) Fuqua, P. D.; Mansour, K.; Alvarez, J. D.; Marder, S. R.; Perry, J. W.; Dunn, B. S. Synthesis and nonlinear optical properties of sol-gel materials containing phthalocyanines. *Proc. SPIE, Sol-Gel Optics II* **1992**, 1758, 499.
- (28) Bentivegna, F.; Canva, M.; Georges, P.; Brun, A.; Chaput, F.; Malier, L.; Boilot, J. P. Reverse saturable absorption in solid xerogel matrices. *Appl. Phys. Lett.* **1993**, 62, 1721-1723.
- (29) Innocenzi, P.; Brusatin, G.; Guglielmi, M.; Signorini, R.; Bozio, R.; Maggini, M. 3-(Glycidoxypropyl)-trimethoxysilane-TiO<sub>2</sub> hybrid organic-inorganic materials for optical limiting. *J. Non-Cryst. Solids* **2000**, 265, 68-74.
- (30) Kopitkovas, G.; Chugreev, A.; Nierengarten, J. F.; Rio, Y.; Rehspringer, J. L.; Hönerlage, B. Reverse saturable absorption of fullerodendrimers in porous SiO<sub>2</sub> sol-gel matrices. *Opt. Mater.* **2004**, 27, 285-291.
- (31) Sanz, N.; Ibanez, A.; Morel, Y.; Baldeck, P. L. Organic nanocrystals grown in gel glasses for optical-power-limiting applications. *Appl. Phys. Lett.* **2001**, 78, 2569-2571.
- (32) Morales-Saavedra, O. G.; Rivera, E. Linear and nonlinear optical properties of trans- and cis-poly(1-ethynylpyrene) based sonogel hybrid materials. *Polymer* **2006**, 47, 5330-5337.
- (33) Desroches, C.; Lopes, C.; Kessler, V.; Parola, S. Design and synthesis of multifunctional thiacalixarenes and related metal derivatives for the preparation of sol-gel hybrid materials with non-linear optical properties. *Dalton Trans.* **2003**, 2085-2092.
- (34) Zieba, R.; Desroches, C.; Chaput, F.; Carlsson, M.; Eliasson, B.; Lopes, C.; Lindgren, M.; Parola, S. Preparation of Functional Hybrid Glass Material from Platinum (II) Complexes for Broadband Nonlinear Absorption of Light. *Adv. Func. Mater.* **2009**, 19, 235-241.
- (35) Chateau, D.; Chaput, F.; Lopes, C.; Lindgren, M.; Brannlund, C.; Ohgren, J.; Djourellov, N.; Nedelec, P.; Desroches, C.; Eliasson, B.; Kindahl, T.; Lerouge, F.; Andraud, C.; Parola, S.

Silica hybrid sol-gel materials with unusually high concentration of Pt-organic molecular guests: studies of luminescence and nonlinear absorption of light. *ACS Appl. Mater. Interfaces* **2012**, *4*, 2369-2377.

(36) Zheng, X.; Feng, M.; Zhan, H. Giant optical limiting effect in Ormosil gel glasses doped with graphene oxide materials. *J. Mater. Chem. C* **2013**, *1*, 6759-6766.

(37) Zheng, C.; Zheng, Y.; Chen, W.; Wei, L. Encapsulation of graphene oxide/metal hybrids in nanostructured sol-gel silica ORMOSIL matrices and its applications in optical limiting. *Opt. Laser Technol.* **2015**, *68*, 52-59.

(37) Chateau, D.; Liotta, A.; Lundén, H.; Lerouge, F.; Chaput, F.; Krein, D.; Cooper, T.; Lopes, C.; Lindgren, M.; Parola, S. Long Distance Enhancement of Nonlinear Optical Properties Using Low Concentration of Plasmonic Nanostructures in Dye Doped Monolithic Sol-Gel Materials. *Adv. Funct. Mater.* **2016**, *26* (33), 6005-6014.

(38) Kumar, P.; Mathpal, M. C. ; Jagannath, G.; Prakash, J. ; Maze, J.-R. ; Roos, W. D.; Swart, H. C. Optical limiting applications of resonating plasmonic Au nanoparticles in a dielectric glass medium, *Nanotechnology* 2021, *32*, 345709-345725

(39) Château, D.; Bellier, Q.; Chaput, F.; Feneyrou, P.; Berginc, G.; Maury, O.; Andraud, C.; Parola, S. Efficient hybrid materials for optical power limiting at telecommunication wavelengths. *J. Mater. Chem. C* **2014**, *2*, 5105-5110.

(40) David, S.; Chateau, D.; Chang, H.-J.; Karlsson, L. H.; Bondar, M. V.; Lopes, C.; Le Guennic, B.; Jacquemin, D.; Berginc, G.; Maury, O.; Parola, S.; Andraud, C. High-Performance Optical Power Limiting Filters at Telecommunication Wavelengths: When Aza-BODIPY Dyes Bond to Sol-Gel Materials. *J. Phys. Chem. C* **2020**, *124* (44), 24344-24350.

- (41) Sharma, S.; Mohan, D.; Ghoshal, S. K. Measurement of nonlinear properties and optical limiting ability of Rhodamine6G doped silica and polymeric samples. *Opt. Commun.* **2008**, *281*, 2923-2929.
- (42) Signorini, R.; Meneghetti, M.; Bozio, R.; Maggini, M.; Scorrano, G.; Prato, M.; Brusatin, G.; Innocenzi, P.; Guglielmi, M. Optical limiting and non linear optical properties of fullerene derivatives embedded in hybrid sol–gel glasses. *Carbon* **2000**, *38*, 1653-1662.
- (43) Brusatin, G.; Guglielmi, M.; Innocenzi, P.; Martucci, A.; Scarinci, G. Materials for Photonic Applications From Sol-Gel. *J. Electroceram.* **2000**, *4*, 151-165.
- (44) Tao, L.; Zhou, B.; Bai, G.; Wang, Y.; Yu, S. F.; Lau, S. P.; Tsang, Y. H.; Yao, J.; Xu, D. Fabrication of covalently functionalized graphene oxide incorporated solid-state hybrid silica gel glasses and their improved nonlinear optical response. *J. Phys. Chem. C* **2013**, *117*, 23108-23116.
- (45) Bouit, P.-A.; Kamada, K.; Fenevrou, P.; Berginc, G.; Toupet, L.; Maury, O.; Andraud, C. Two-Photon Absorption-Related Properties of Functionalized BODIPY Dyes in the Infrared Range up to Telecommunication Wavelengths. *Adv. Mater.* **2009**, *21 (10-11)*, 1151-1154.
- (46) Navarro, J. R.G.; Manchon, D.; Lerouge, F.; Cottancin, E.; Lermé, J.; Bonnet, C.; Chaput, F.; Mosset, A.; Pellarin, M.; Parola, S. Synthesis, electron tomography and single-particle optical response of twisted gold nano-bipyramids. *Nanotechnology* **2012**, *23*, 145707.
- (47) Chateau, D.; Liotta, A.; Vadcard, F.; Navarro, J. R. G.; Chaput, F.; Lermé, J.; Lerouge, F.; Parola, S. From gold nanobipyramids to nanojavelins for a precise tuning of the plasmon resonance to the infrared wavelengths: experimental and theoretical aspects. *Nanoscale* **2015**, *7*, 1934-1943.

- (48) Chateau, D.; Desert, A.; Lerouge, F.; Landaburu, G.; Santucci, S.; Parola, S. Beyond the Concentration Limitation in the Synthesis of Nanobipyramids and Other Pentatwinned Gold Nanostructures. *ACS Appl. Mater. Interfaces* **2019**, *11*, 42, 39068-39076.
- (49) Lundén, H.; Liotta, A.; Chateau, D.; Lerouge, F.; Chaput, F.; Parola, S.; Brännlund, C.; Ghadyani, Z.; Kildemo, M.; Lindgren, M.; Lopes, C. Dispersion and self-orientation of gold nanoparticles in sol–gel hybrid silica – optical transmission properties. *J. Mater. Chem. C* **2015**, *3*, 1026-1034.
- (50) Pascal, S.; Bellier, Q.; David, S.; Bouit, P.-A.; Chi, S.-H.; Makarov, N. S.; Le Guennic, B.; Chibani, S.; Berginc, G.; Feneyrou, P.; Jacquemin, D.; Perry, J. W.; Maury, O.; Andraud, C. Unraveling the Two-Photon and Excited-State Absorptions of Aza-BODIPY Dyes for Optical Power Limiting in the SWIR Band. *J. Phys. Chem. C* **2019**, *123* (38), 23661-23673.
- (51) Chateau, D.; Liotta, A.; Gregori, D.; Lerouge, F.; Chaput, F.; Desert, A.; Parola, S. Controlled surface modification of gold nanostructures with functionalized silicon polymers. *J. Sol-Gel Sci. Technol.* **2017**, *81*, 147-153.
- (52) (Thesis) Lundén H. Nonlinear materials for optical power limiting: characterization and modelling. *PhD Thesis*, Linköping University (Linköping, Sweden), May, **2019**.

SYNOPSIS (Word Style "SN\_Synopsis\_TOC").

